2. J. D. Gralla, *Cell* **66**, 415 (1991); S. Sasse-Dwight and J. D. Gralla, *ibid.* **62**, 945 (1990); Y. Tintut, J. Wang, J. D. Gralla, *Genes Dev.* **9**, 2305 (1995).
3. C. Wong, Y. Tintut, J. D. Gralla, *J. Mol. Biol.* **236**, 81 (1994); Y. Tintut, C. Wong, Y. Jiang, M. Hsieh, J. D. Gralla, *Proc. Natl. Acad. Sci. U.S.A.* **91**, 2120 (1994).
4. M. Hsieh and J. D. Gralla, *J. Mol. Biol.* **239**, 15 (1994).
5. M. Hsieh, Y. Tintut, J. D. Gralla, *J. Biol. Chem.* **269**, 373 (1994).
6. L. Ray, F. Claverie-Martin, P. Weglenski, B. Magasanik, *J. Bacteriol.* **172**, 818 (1990).
7. A. Syed, B. Wolner, J. D. Gralla, unpublished data.
8. Wild-type σ protein was purified as described [(D. Popham, J. Keener, S. Kustu, *J. Biol. Chem.* **266**, 19510 (1991)]. The mutant σ^{54} proteins were cloned into plasmid pJF5401 [B. Schauder, H. Blöcker, R. Grank, J. E. G. McCarthy, *Gene* **52**, 279 (1987)] and induced by shifting the temperature to 42°C for 4 hours. The mutant proteins were found in inclusion bodies, and therefore the insoluble fraction after cell disruption was taken. This fraction was dissolved in buffered 4 M guanidium HCl and 0.1% NP-40 nonionic detergent, dialyzed into 1 M guanidium and then into buffer without guanidium. Subsequent chromatography was as described for the wild-type protein. After three column purification steps, the proteins were >90% pure.
9. The standard in vitro transcription reaction contained 5 nM supercoiled DNA template pYS1 bearing the *glnAp2* promoter, 100 nM NtrC purified as described [J. B. Moore, S. P. Shiau, L. J. Reitzer, *J. Bacteriol.* **175**, 2692 (1993); the concentration used was determined by titration], 10 mM carbamyl phosphate [J. Feng *et al., ibid.* **174**, 6061 (1992)], 100 nM σ^{54}, 1 unit *E. coli* RNA core polymerase (Epicentre Technology, Madison, WI), and 0.5 mM each nucleotide triphosphate (NTP), except ATP at 3 mM, in transcription buffer [50 mM Tris (pH 7.8), 100 mM KCl, 10 mM $MgCl_2$, 0.1 mM EDTA, 1 mM dithiothreitol, bovine serum albumin (50 ng), and 3.5% (w/v) polyethylene glycol] in a 40-μl reaction volume. All components were assembled on ice, and after addition of NTP the reactions were incubated at 37°C for 6 to 7 min. Reactions were stopped by adding an equal volume of 5 M NH_4OAc and 100 mM EDTA. The RNA transcript was ethanol-precipitated and then subjected to primer extension with reverse transcriptase (Promega) and the ^{32}P-labeled oligonucleotide downstream primer described in (*3*). The radioactive extension product was separated on a 10% urea polyacrylamide gel and visualized by autoradiography.
10. A. Ninfa, L. J. Reitzer, B. Magasanik, *Cell* **50**, 1039 (1987).
11. Twofold to threefold stimulation of transcription with σ mutants occurs at high concentrations of NtrC (J. T. Wang and J. D. Gralla, unpublished data).
12. S. Kustu, A. K. North, D. S. Weiss, *Trends Biochem. Sci.* **16**, 397 (1991); W. Wang, M. Carey, J. D. Gralla, *Science* **255**, 450 (1992).
13. D. S. Weiss, J. Batut, K. E. Klose, J. Keener, S. Kustu, *Cell* **67**, 155 (1991).
14. Standard in vitro transcription reactions were assembled except for LS2633, where NtrC, carbamyl phosphate, and the high concentration of ATP were omitted. Samples were taken from the reaction at various times. The primer extension product of the RNA was visualized and quantified by direct phosphorimaging.
15. W. Su, S. Porter, S. Kustu, H. Echols, *Proc. Natl. Acad. Sci. U.S.A.* **87**, 5504 (1990).
16. C. A. Gross, M. Lonetto, R. Losick, in *Transcriptional Regulation,* S. L. McKnight and K. R. Yamamoto, Eds. (Cold Spring Harbor Laboratory Press, Cold Spring Harbor, NY, 1992), pp. 129–176.
17. D. L. Popham, D. Szeto, J. Keener, S. Kustu, *Science* **243**, 629 (1989).
18. Y. Tintut, J. T. Wang, J. D. Gralla, *J. Biol. Chem.* **270**, 24392 (1995).
19. Potassium permanganate footprinting was done under the conditions of in vitro transcription, except that the supercoiled DNA template was at 1 nM, KCl was at 20 mM, and Hepes replaced Tris buffer. Other details are as described in (*18*).
20. We thank A. Ninfa and J. Moore for expression plasmids; Y. Tintut, H. Cai, and Y. Song for their help; and A. J. Courey and J. Gober for advice. Supported by NIH grant GM35754. M.H. was supported in part by grants NSC84-2331-B-040-008 and CSMC 83-NS-A-047 from the government of Taiwan.

7 June 1995; accepted 14 September 1995

Transition in Specification of Embryonic Metazoan DNA Replication Origins

Olivier Hyrien,*† Chrystelle Maric,† Marcel Méchali*

In early *Xenopus* embryos, in which ribosomal RNA genes (rDNA) are not transcribed, rDNA replication initiates and terminates at 9– to 12–kilobase pair intervals, with no detectable dependence on specific DNA sequences. Resumption of ribosomal RNA (rRNA) synthesis at late blastula and early gastrula is accompanied by a specific repression of replication initiation within transcription units; the frequency of initiation within intergenic spacers remains as high as in early blastula. These results demonstrate that for rRNA genes, circumscribed zones of replication initiation emerge in intergenic DNA during the time in metazoan development when the chromatin is remodeled to allow gene transcription.

Eukaryotic DNA replication initiates at multiple replication origins spread along the length of each chromosome. In yeast, replication origins correspond to specific nucleotide sequences (*1*). In higher eukaryotes, the nature of replication origins is much less clear. For example, initiation can occur at any of a large number of sites in a 55-kbp zone downstream of the Chinese hamster dihydrofolate reductase (DHFR) gene, even though some sites may be preferred (*2–4*). Several other studies have suggested a lack of specific origin sequences in metazoan cells (*1*, *2*). On the other hand, replication of the human β-globin gene cluster may be regulated by a DNA sequence located between the δ- and β-globin genes (*5*).

The tandemly repeated, highly conserved rRNA genes (Fig. 1A) provide an interesting model of eukaryotic replicons. Electron microscopy studies of replicating DNA or chromatin have long suggested that initiation is restricted to the rDNA intergenic spacer in many protozoan and metazoan species [references in (*6*, *7*)]. Analysis of replication intermediates (RIs) by two-dimensional (2D) gel electrophoresis confirmed that replication initiates in the rDNA spacer, the noncoding sequences between genes, at specific sites in *Saccharomyces cerevisiae* (*8*, *9*) and *Physarum polycephalum* (*6*) and in a broad zone in human cells (*10*). A replication fork barrier was also found at the 3′ end of ribosomal genes in several species (*7–11*).

Molecular Embryology, Institut Jacques Monod, 75 251 Paris Cedex 05, France.

*To whom correspondence should be addressed.
†Present address: Génétique Moléculaire, Département de Biologie, Ecole Normale Supérieure, 46 rue d'Ulm, 75230 Paris Cedex 05, France.

In contrast to this conserved pattern of fixed sites or zones of initiation and termination, replication initiates and terminates at random sequences, though at regular 9- to 12-kbp intervals, in the rDNA of *Xenopus* early blastulae (*12*). Plasmids containing the *Xenopus* rDNA sequences also showed random initiation and termination of DNA replication in *Xenopus* eggs or egg extracts (*13*, *14*). An important difference with the other experimental systems is that transcription of the zygotic genome, including rRNA genes (*15*), is repressed in eggs and early embryos. In order to analyze the relation between transcription and replication at this locus, we investigated whether resumption of rRNA synthesis after the *Xenopus* mid-blastula transition is accompanied by changes in chromosomal rDNA replication.

RIs of the restriction fragments (Fig. 1A) were analyzed by 2D gel electrophoresis (Fig. 1C). The principle of this technique is to resolve replication fork–containing restriction fragments according to both mass and shape (*16*) (Fig. 1B). The relative amounts of bubbles, double forks, and simple forks of a given fragment reflect the frequencies of initiation and termination within that fragment.

At the mid-blastula stage, each restriction fragment showed a strong bubble arc, a simple fork arc, and a double fork triangular smear, indicating that initiation and termination occur at multiple positions throughout rDNA repeats. These patterns are essentially similar to those we found previously for the early blastula stage (*12*).

At later stages, the ratio of bubbles to simple forks was visibly decreased in fragments B, C, D, and E but not in fragment A. RIs were measured on a PhosphorImager

in order to quantitate these changes in several independent experiments and to estimate the frequency of initiation and termination within each fragment at each stage. These frequencies are defined as the number of events per kilobase pair of DNA sequence, and their calculation takes into account the size of the fragment as well as the percentage of its various RIs (*12*, *17*) (Table 1 and Fig. 2). The frequency of initiation in fragments B, C, D, and E decreased by a factor of 2 to 5 from early blastula to early gastrula (Fig. 2). The decrease was sharper between mid- and late blastula. In contrast, the frequency of initiation in fragment A increased 1.4-fold during the same time period. It is important to remember that the portion of a fragment where bubbles can be reliably detected is limited to its inner third (*18*). Therefore, (i) the reduction of initiation observed for fragments B, C, D, and E affects the complete transcription unit and (ii) the only sequences of the A fragment that contribute to its bubble arc are approximately those belonging to the right half of the intergenic spacer. The low incidence of bubbles in the C and D fragments implies a reduction of initiation over the edges, but not the center, of the A fragment.

The ratio of initiation frequency in transcription units relative to intergenic spacers was calculated for each developmental stage by analyzing the same DNA sample on the same blot with the two Eco RI probes A and B (Fig. 3). This normalization eliminated any potential artefact caused by unequal RI losses in different experiments. The frequency of initiation was nearly the same in the intergenic spacers (fragment A) and in the transcription units (fragment B) at early blastula, but decreased progressively in transcription units relative to spacers (to one-third of the original value) as development proceeded. The decrease in fragments C and D appeared even stronger than in fragment B (Fig. 2).

We conclude that from mid-blastula to early gastrula, replication initiation became repressed in the precursor rRNA coding sequences but continued in the intergenic spacer at a similar or slightly higher frequency than at early blastula. This origin specification resulted in a moderate (a factor of about 1.7) decrease in origin density (calculated as the size-weighted average of initiation frequency within fragments A, B, C, and D). Average origin density in total genomic DNA is much lower in adult *Xenopus* cells than in embryos (*19*), but it has not been measured specifically within adult rDNA, and it is possible that rDNA replicons, unlike other genomic replicons, do not further increase in size during later development. Note that a residual level of initiation could still be detected within transcription units. A similar low level of initiation in transcription units was recently reported for two other initiation zones in adult mammalian cells (*20*), including that of human rDNA. It is therefore possible that the origin site of *Xenopus* rRNA genes does not become further restrictive during development. Two-dimensional gel analysis of *Xenopus* rDNA in differentiated cells has yet to reach a higher sensitivity than previ-

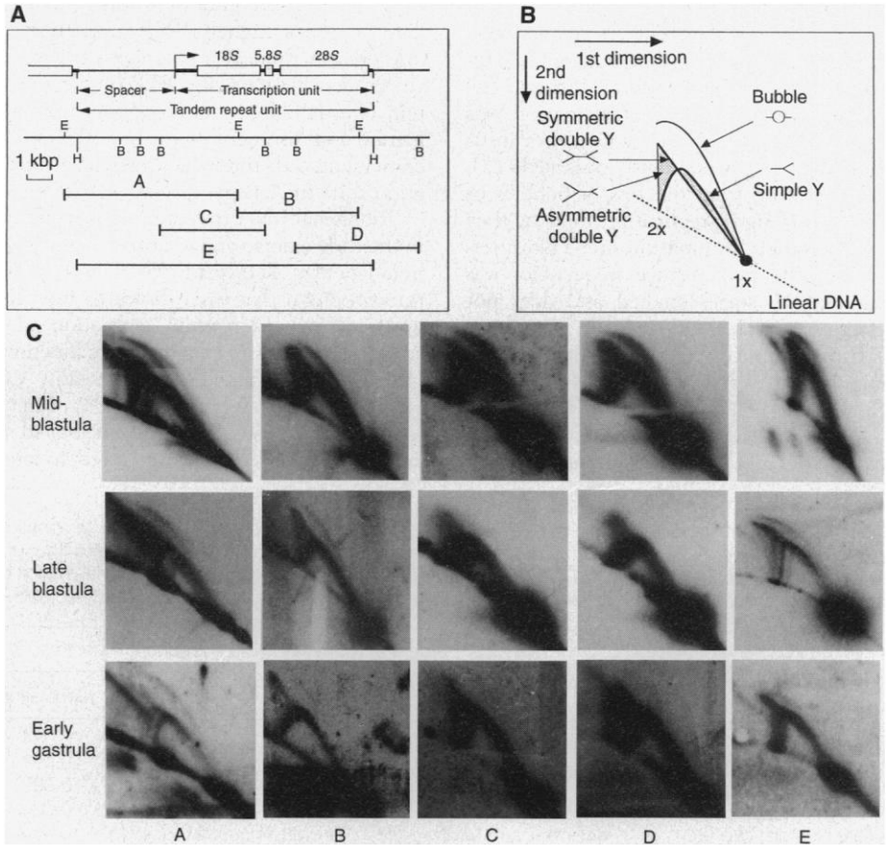

Fig. 1. Two-dimensional gel electrophoretic analysis of *Xenopus* rDNA replication intermediates. (**A**) Organization of *X. laevis* rDNA repeat unit, restriction map, and restriction fragments used in this study. E, Eco RI; B, Bam HI; H, Hind III. (**B**) Diagram of 2D gel electrophoretic patterns (*16*) generated by the three basic forms of replication fork–containing restriction fragments. Fragments are separated according to mass (that is, replication extent) in the first dimension and to shape in the second dimension. Thus, single forks (simple forks, or Y) are resolved from fragments with two diverging forks (bubbles, or O) or two converging forks (double forks, or H). Blot analysis of overlapping fragments enables deduction of the position of replication initiation and termination sites within the mapped locus (*13*, *16*). (**C**) Replication intermediates of fragments A to E from mid-blastula (8000 cells), late blastula (16,000 cells), and early gastrula (32,000 cells) embryos. Replication intermediates cut with Bam HI, Eco RI, or Hind III were prepared as described (*12*), with a further purification on benzyl-naphtyl-DEAE cellulose chromatography (*29*). Two-dimensional gel electrophoresis, blotting, and hybridization were done as described (*12*).

Fig. 2. Changes in the frequency of replication initiation and termination within rDNA restriction fragments A, B, C, D, and E. Mean values and standard errors calculated from the data in Table 1 were plotted against developmental stage. (□) Fragment A, (◇) fragment B, (○) fragment C, (△) fragment D, and (⊞) fragment E.

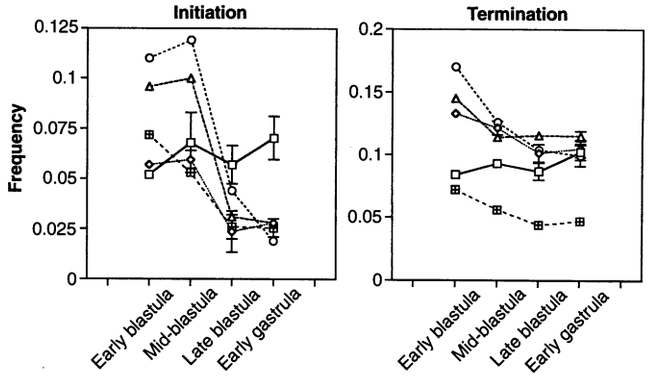

ously achieved (*11*), in order to address these questions and to allow direct comparison with transcription and chromatin structure data (*21*).

In contrast to the rDNA origin specification, termination events became uniformly distributed along the rDNA repeats at early gastrula. Double forks were still detected everywhere, but in smaller percentages, consistent with a moderately larger replicon size (Figs. 1 and 2). Intriguingly, the average frequency of termination was higher than the average frequency of initiation (Fig. 2). As previously observed (*12*), this may arise from the loss of bubbles or from a slowing of replication forks as they approach their termination site. This difference in the two average frequencies was found at all stages studied and does not affect our conclusions.

Strong replication fork barriers (RFBs) have been observed in the rDNA of yeast (*8*, *9*), pea (*7*), human (*10*), or *Xenopus* (*11*) cultured cells. Short exposures of the fork arc of the D fragment, either before or after the mid-blastula, revealed only a weak discontinuity, suggesting that only a minority of forks slow down at the 3′ end of the transcription unit (*22*). A peculiar DNA structure may slow progression of some forks independently of rRNA transcription. However, the later establishment of a point at which progression of most forks is halted may require a higher rRNA transcription rate or formation of a complex with an as yet unidentified specific RFB-binding protein (*11*, *12*). In conclusion, the developmental establishment of a strong RFB is not coincident with that of a preferential initiation zone in *Xenopus* rDNA.

Ribosomal RNA transcription is repressed in the early embryo and resumes progressively from late blastula onward (*15*). Transcription through origins has been shown to interfere with autonomous plasmid replication (*23*) and may in itself suppress origin function. However this hypothesis cannot easily explain our results. At least 75 to 80% of transcription units would need to be activated at late blastula to account for the three- to four-fold repression of replication initiation within transcription units that we observed. The proportion of active units in these embryos, which slowly resume transcription (*15*), is certainly lower (0 to 25%), because in actively transcribing cultured cells this proportion is only 25% (*21*). The formal possibility that at late blastula a high proportion of rRNA genes would be transcribed, but at a low rate, seems unlikely because in all systems thus far studied (*21*), each rRNA gene appears either inactive or fully active. Furthermore, in *X. laevis*, all intergenic spacers downstream of active genes are mostly or entirely transcribed by RNA polymerase I as a result of inefficient transcription termination at the 3′ end of the gene (*21*, *24*). Interestingly, recent reports of metazoan replication origins within expressed genes show that transcription does not necessarily interfere with replication initiation (*25*).

The confinement of DNA replication initiation to circumscribed zones may be related to the determination of a locus for transcription rather than to the actual, high-level transcription of the gene. The inner third of the A fragment contains a complex battery of repeated promoter and enhancer elements that can bind the rRNA transcription factor UBF (*26*). Transcription factors can stimulate animal virus replication independently of transcription (*27*), and intergenic DNA-bound UBF may act similarly and facilitate access by the replication initiation machinery after the mid-blastula transition. Whether this origin specification subsequently helps to activate rRNA transcription remains to be explored. Nevertheless, the role of transcription factors in viral DNA replication need not reflect the controls imposed on cellular DNA replication. Alternatively, some chromatin remodeling after the mid-blastula transition, distinct from the active process of transcription, might distinguish transcription units from intergenic regions and render them refractory to replication initiation.

Table 1. Quantitation of replication intermediates (RIs) and calculations of initiation and termination frequencies. RIs were quantitated on a PhosphorImager and corrected for partial overlap, and frequencies were calculated, as described (*12*, *17*). Data for early blastula are from (*12*). The variable size of fragments A, C, D, and E is due to length polymorphism of the intergenic spacer. ND, not detectable.

Fragment and stage	Fragment size (kbp)	Percent of total RIs			Frequency (per kbp) of	
		O	H	Y	initiation	termination
A (early blastula)	7.5– 8.5	9.1	33.2	57.7	0.052	0.084
A (mid-blastula, exp. 1)	7.0– 9.0	19.9	35.4	44.7	0.083	0.093
A (mid-blastula, exp. 2)	6.4– 8.8	8.0	38.0	54.0	0.053	0.093
A (late blastula, exp. 1)	7.0– 9.5	10.8	40.0	49.2	0.060	0.090
A (late blastula, exp. 2)	6.9– 8.4	12.2	36.5	51.3	0.067	0.093
A (late blastula, exp. 3)	7.5– 9.0	7.8	30.0	62.2	0.044	0.077
A (early gastrula, exp. 1)	7.0– 8.0	13.5	40.0	46.5	0.078	0.103
A (early gastrula, exp. 2)	7.0– 8.0	8.1	42.3	49.6	0.055	0.094
A (early gastrula, exp. 3)	6.9– 8.5	17.1	32.9	50.0	0.078	0.110
B (early blastula)	4.9	5.3	32.6	62.1	0.057	0.133
B (mid-blastula, exp. 1)	4.9	7.0	25.0	68.0	0.064	0.116
B (mid-blastula, exp. 2)	4.9	5.4	29.8	64.8	0.055	0.127
B (late blastula, exp. 1)	4.9	3.4	24.0	72.6	0.035	0.111
B (late blastula, exp. 2)	4.9	2.5	20.2	77.3	0.026	0.099
B (late blastula, exp. 3)	4.9	1.5	19.2	80.5	0.016	0.094
B (early gastrula, exp. 1)	4.9	2.7	25.0	72.3	0.029	0.112
B (early gastrula, exp. 2)	4.9	2.6	19.8	77.6	0.027	0.098
C (early blastula)	4.2	10.1	36.9	52.9	0.110	0.170
C (mid-blastula)	4.1– 4.2	14.4	20.5	65.1	0.119	0.126
C (late blastula, exp. 1)	4.2	4.0	16.5	79.5	0.044	0.102
C (late blastula, exp. 2)	4.4– 4.6	ND	20.2	79.8	ND	0.106
C (early gastrula, exp. 1)	4.3– 4.5	1.7	15.5	82.8	0.019	0.091
C (early gastrula, exp. 2)	4.3– 5.0	ND	21.9	78.1	ND	0.108
D (early blastula)	4.5	10.0	30.9	59.1	0.096	0.145
D (mid-blastula)	4.5	12.4	19.7	67.9	0.100	0.114
D (late blastula, exp. 1)	4.5	2.7	23.5	73.8	0.031	0.119
D (late blastula, exp. 2)	4.5	ND	22.0	78.0	ND	0.112
D (early gastrula, exp. 1)	4.5– 4.8	2.4	25.3	72.3	0.028	0.119
D (early gastrula, exp. 2)	4.3– 4.7	ND	23.3	76.7	ND	0.111
E (early blastula)	12.7–14.2	31.7	63.6	4.7	0.072	0.072
E (mid-blastula)	12.0–13.5	21.4	32.7	45.9	0.053	0.056
E (late blastula, exp. 1)	13.5–15.0	11.4	27.7	60.9	0.032	0.044
E (late blastula, exp. 2)	13.0–15.0	5.6	29.3	65.1	0.020	0.044
E (early gastrula, exp. 1)	10.0–12.0	7.9	22.2	69.9	0.030	0.048
E (early gastrula, exp. 2)	12.5–13.5	5.6	26.7	67.7	0.021	0.046

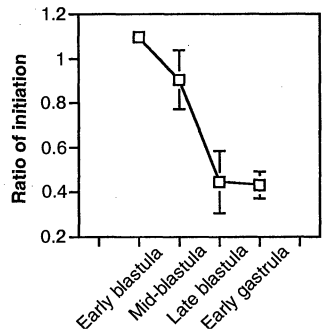

Fig. 3. Changes in the ratio of initiation in fragment B relative to fragment A. Both probes were used to analyze the same DNA sample on the same blot for each developmental stage. The mean ratios and standard errors were calculated from the data in Table 1.

In either model, the apparent sequence specificity of some metazoan replication origins would result from modulation by the nuclear context of a primarily nonsequence-specific initiation mechanism. Indeed, *Xenopus* egg extracts are able to initiate DNA replication specifically within the Chinese hamster DHFR initiation zone if intact G_1-phase nuclei are used as the substrate (*28*). This finding was suggested to result from nuclear structure rather than transcription, although it remains to be demonstrated that *Xenopus* egg extracts do not carry out transcription in these experiments.

The confinement of replication initiation outside of genes may have had different evolutionary consequences in organisms with different ways of life (*1*, *12*). Protozoa and viruses with small genomes, little intergenic DNA, and requirements for rapid growth could have been favored by the emergence of efficient, sequence-specific replication origins. On the contrary, a non–sequence-specific initiation mechanism may adapt with greater flexibility to the variety of proliferation rates and nuclear contexts found in a metazoan organism.

REFERENCES AND NOTES

1. B. J. Brewer, *Curr. Opin. Genet. Dev.* **4**, 196 (1994).
2. J. L. Hamlin and P. A. Dijkwell, *ibid.* **5**, 153 (1995).
3. J. P. Vaughn, P. A. Dijkwell, J. L. Hamlin, *Cell* **61**, 1075 (1990); P. A. Dijkwell and J. L. Hamlin, *Mol. Cell. Biol.* **15**, 3023 (1995).
4. W. C. Burhans, L. T. Vassilev, M. S. Caddle, N. H. Heintz, M. L. DePamphilis, *Cell.* **62**, 955 (1990).
5. D. Kitsberg, S. Selig, I. Keshet, H. Cedar, *Nature* **366**, 588 (1993).
6. M. Bénard, C. Lagnel, G. Pierron, *Nucleic Acids Res.* **23**, 1447 (1995).
7. P. Hernandez, L. Martin-Parras, M. L. Martinez-Robles, J. B. Schvartzman, *EMBO J.* **12**, 1475 (1993).
8. B. J. Brewer and W. L. Fangman, *Cell* **55**, 637 (1988).
9. M. H. K. Linskens and J. A. Huberman, *Mol. Cell. Biol.* **8**, 4927 (1988).
10. R. D. Little, T. H. K. Platt, C. Schildkraudt, *ibid.* **13**, 6600 (1993).
11. B. Wiesendanger, R. Lucchini, T. Koller, J. Sogo, *Nucleic Acids Res.* **22**, 5038 (1994).
12. O. Hyrien and M. Méchali, *EMBO J.* **12**, 4511 (1993).
13. ———, *Nucleic Acids Res.* **20**, 1463 (1992).
14. H. M. Mahbubani, T. Paull, J. K. Elder, J. J. Blow, *ibid.*, p. 1457.
15. K. Shiokawa, Y. Misumi, K. Yamana, *Dev. Growth Differ.* **23**, 579 (1981).
16. B. J. Brewer and W. L. Fangman, *Cell* **51**, 463 (1987).
17. The frequencies of initiation (F_i) or termination (F_t) (number of events per kilobase pair of DNA sequence within each fragment) are here defined as

$$F_i = 1/n[1 + (2/9)(Y/O)] \quad (1)$$

$$F_t = 1/n[1 + (5/18)(Y/H)] \quad (2)$$

where n is the size of the fragment analyzed, and O, H, and Y are the percentages of bubbles, double forks, and simple forks, respectively. These formulas were derived assuming random initiation and termination and constant fork speed within the fragment (*12*). If initiation and termination occur with different efficiencies along the DNA sequences, these formulas tend to underestimate the actual differences between fragments (calculations not shown). Therefore, they remain valid approximations for the present study. Results from identical experiments (Table 1) varied by less than ±9% for termination frequency but up to ±30% for the lowest initiation frequencies. Only much larger changes over development are discussed here. When, due to size polymorphism, Y's of larger fragments overlapped with H's of smaller fragments, we corrected the respective signals by subtracting from Y's and adding to H's the contribution of H's to the zone of overlap. This value was estimated from the area of the overlap zone and from the average signal in immediately adjacent H's free of Y's.
18. M. H. K. Linskens and J. A. Huberman, *Nucleic Acids Res.* **18**, 647 (1988).
19. H. G. Callan, *Proc. R. Soc. London Ser. B.* **181**, 19 (1972).
20. Y. Yoon, J. A. Sanchez, C. Brun, J. A. Huberman, *Mol. Cell. Biol.* **15**, 2482 (1995); P. A. Dijkwell, J. P. Vaughn, J. L. Hamlin, *Nucleic Acids Res.* **22**, 4989 (1994).
21. R. Lucchini and J. M. Sogo, *Mol. Cell. Biol.* **12**, 4288 (1992).
22. O. Hyrien, C. Maric, M. Mechali, data not shown; but see figure 4D in (*12*).
23. S. B. Haase, S. S. Heinzel, M. P. Calos, *Mol. Cell. Biol.*. **14**, 2516 (1994). W.-J. Pan, R. C. Gallagher, E. H. Blackburn, *ibid.* **15**, 3372 (1995); M. Snyder, R. J. Sapolsky, R. W. Davis, *ibid.* **8**, 2184 (1988).
24. R. F. J. De Winter and T. Moss, *Nucleic Acids Res.* **14**, 6041 (1986); P. Labhart and R. H. Reeder, *Cell* **45**, 431 (1986).
25. C. Wu, M. Zannis-Hadjopoulos, G. B. Price, *Biochim. Biophys. Acta* **1174**, 258 (1993); E. S. Tasheva and D. J. Roufa, *Mol. Cell. Biol.* **14**, 5628 (1994); R. E. Kelly, M. L. DeRose, B. W. Draper, G. M. Wahl, *ibid.* **15**, 4136 (1995).
26. R. H. Reeder, *Trends Genet.* **6**, 390 (1990).
27. M. L. DePamphilis, *Trends Cell Biol.* **3**, 161 (1993).
28. D. M. Gilbert, H. Miyazawa, M. L. DePamphilis, *Mol. Cell. Biol.* **15**, 2942 (1995).
29. P. A. Dijkwell, J. P. Vaughn, J. L. Hamlin, *ibid.* **11**, 3850 (1991).

30. We thank S. Bocquet for help with embryo collection and P. Brooks, G. Pierron, Y. Vassetsky, and P. Hughes for critical reading of the manuscript. Supported by grants from INSERM, the Association pour la Recherche sur le Cancer, the European Community, and the Ligue Nationale Française contre le Cancer.

2 May 1995; accepted 19 September 1995

A Left-Handed Parallel β Helix in the Structure of UDP-*N*-Acetylglucosamine Acyltransferase

Christian R. H. Raetz and Steven L. Roderick*

UDP-*N*-acetylglucosamine 3-*O*-acyltransferase (LpxA) catalyzes the transfer of (*R*)-3-hydroxymyristic acid from its acyl carrier protein thioester to UDP-*N*-acetylglucosamine. LpxA is the first enzyme in the lipid A biosynthetic pathway and is a target for the design of antibiotics. The x-ray crystal structure of LpxA has been determined to 2.6 angstrom resolution and reveals a domain motif composed of parallel β strands, termed a left-handed parallel β helix (LβH). This unusual fold displays repeated violations of the protein folding constraint requiring right-handed crossover connections between strands of parallel β sheets and may be present in other enzymes that share amino acid sequence homology to the repeated hexapeptide motif of LpxA.

The outermost membrane monolayer of Gram-negative bacteria is composed primarily of the lipid A moiety of lipopolysaccharide (LPS). The first step of lipid A biosynthesis in *Escherichia coli* is catalyzed by the cytosolic enzyme LpxA, which acts specifically to transfer the 14-carbon fatty acid, (*R*)-3-hydroxymyristate, from its acyl carrier protein thioester to the 3′-OH position of UDP-*N*-acetylglucosamine (*1*). LpxA and other enzymes of lipid A biosynthesis are essential for bacterial growth, as well as the maintenance of the permeability barrier function of the outer membrane (*2*).

The *lpxA* gene from *E. coli* has been cloned and encodes a subunit of 262 residues (*3*). The amino acid sequence is similar to that of several other enzymes, most of which are bacterial acetyl- and acyltransferases (*4*–*6*), including the enzyme that catalyzes the third step of lipid A biosynthesis, UDP-3-*O*-(*R*-3-hydroxymyristoyl)-glucosamine *N*-acyltransferase (LpxD; FirA) (*7*). The region of sequence similarity common to all of these enzymes is a tandem-repeated imperfect six-residue sequence motif termed a "hexapeptide repeat" (*6*) or an "isoleucine patch" (*5*). This motif is characterized by an aliphatic residue at every sixth position (usually Ile, Val, or Leu) and a small residue (Ala, Ser, Cys, Val, Thr, or Asn) preceding the hydrophobic residue at position i-2. Glycine often occupies the position immediately after the aliphatic residue position. The hexapeptide repeat sequence motif occurs 28 times in LpxA within the NH_2-terminal 186 residues.

The x-ray crystal structure of LpxA was solved by the method of isomorphous replacement with two heavy-atom derivatives and refined to a conventional *R* factor of 18.4% at 2.6 Å resolution (*8*, *9*). Crystallographic statistics are presented in Table 1. The atomic model reveals that LpxA is a trimer composed of three identical subunits that are related by a crystallographic three-fold rotation axis (Fig. 1). Each subunit is composed of two domains: an NH_2-terminal domain of predominantly parallel β-sheet structure (residues 1 to 186) and a COOH-terminal domain (residues 187 to 262) containing four α helices. The polypeptide

C. R. H. Raetz, Department of Biochemistry, Duke University Medical Center, Durham, NC 22710, USA.
S. L. Roderick, Department of Biochemistry, Albert Einstein College of Medicine, Bronx, NY 10461, USA.

*To whom correspondence should be addressed.